Chinese Chemical Letters 34 (2023) 108110

Contents lists available at ScienceDirect

Chinese Chemical Letters

journal homepage: www.elsevier.com/locate/cclet

An integrated microfluidic device for the simultaneous detection of multiple antibiotics

Xiaorui Wang[a], Gaowa Xing[b], Nan Li[c], Yaoshuang Xie[a], Ling Lin[a,*]

[a] Department of Bioengineering, Beijing Technology and Business University, Beijing 100048, China
[b] College of Chemistry and Chemical Engineering, Lanzhou University, Lanzhou 730000, China
[c] School of Chinese Materia Medica, Beijing University of Chinese Medicine, Beijing 100029, China

ARTICLE INFO

Article history:
Received 11 October 2022
Revised 13 December 2022
Accepted 27 December 2022
Available online 29 December 2022

Keywords:
Residual antibiotics
Microfluidic chip
Cruciform valves
Point-of-care-testing (POCT)
Simultaneous detection

ABSTRACT

Residual antibiotics in food pose a serious long-term threat to human health. Therefore, an on-site visualization method for antibiotic detection is required. However, the requirements of traditional antibiotic testing methods in terms of operator proficiency and equipment cost hinder the rapid point-of-care-testing detection of suspected samples. Herein, we reported an integrated microfluidic device combining a microfluidic chip containing cruciform valves with immunochromatographic strips for the rapid detection of multiple antibiotics in milk. The rapid qualitative and quantitative analysis of four types of antibiotics (sulfonamides, β-lactams, streptomycin, and tetracyclines) was performed using mobile phone photography and mobile phone application analysis. The detection time was maintained at 10 min. The limits of detection (LODs) for the four antibiotics were 0.15, 0.12, 0.25, and 0.29 ng/mL, respectively, and the selectivity for the different antibiotics was observed even in a highly complex matrix. This device successfully integrated separation and real-time detection onto a chip and might provide a promising perspective for the detection of multiple antibiotics in milk.

The misuse of antibiotics is a significant public health problem that negatively affects food quality and, in turn, human health. Antibiotic abuse has caused environmental pollution and the accumulation of antibiotic residues in human food and poses an invisible threat to human health [1–5]. In particular, antibiotic residues in milk have a particularly marked impact on the growth of infants and young children, and there is a significant association between early life antibiotic exposure and certain childhood-onset diseases [6]. The European Union and World Health Organization (WHO) have stipulated maximum residue limits (MRLs) for the levels of veterinary drugs in food [7]. Therefore, it is imperative to establish a method for the rapid detection of multiple antibiotic residues in food. Traditional detection methods for antibiotics in milk include liquid or gas chromatography-tandem mass spectrometry, surface-enhanced Raman scattering, and enzyme-linked immunosorbent assays (ELISAs) [8–12]. These methods are costly, time- and reagent-consuming, and complex in terms of processing steps and require specialized operators. Thus, there is an urgent need to develop an automated, simultaneous, and quantifiable platform to detect antibiotics in milk and ensure food safety.

Microfluidic technology has been widely employed for the detection of pathogens and pesticide residues in various fields, such as healthcare, environmental monitoring, and food safety, owing to its high throughput, low cost, and portability for drug screening [13–16]. As a detection device, microfluidic chips can be combined with various detection techniques, such as mass spectrometry, optical detection, electrochemical detection, and biosensors. In the past decade, numerous efforts have been made to develop various on-chip rapid detection methods. In the field of food safety, the combination of microfluidic technology with aptamer sensors, nanocatalysts, and immunoluminescent techniques enables the high-throughput and rapid detection of antibiotics, pathogens, heavy metals, and proteins [17–20]. Depending on the design, different elements, such as pumps, columns, and valves, can be integrated into a microfluidic device, allowing for the entry of gasses, precise reactions, mixing, and flow of reagents [21,22]. These elements can be used in a small chip with multiple reactions. The reagent, sample, and time costs are reduced using microfluidic chips [22–24]. Microfluidic devices can be used for the rapid detection of foodborne pathogenic bacteria and antibiotics, and the detection time can be reduced to less than 10 min [25,26]. However, few rapid and portable field detection methods can simultaneously detect multiple antibiotics in food and perform rapid qualitative and quantitative analysis.

* Corresponding author.
E-mail address: linling@btbu.edu.cn (L. Lin).

https://doi.org/10.1016/j.cclet.2022.108110
1001-8417/

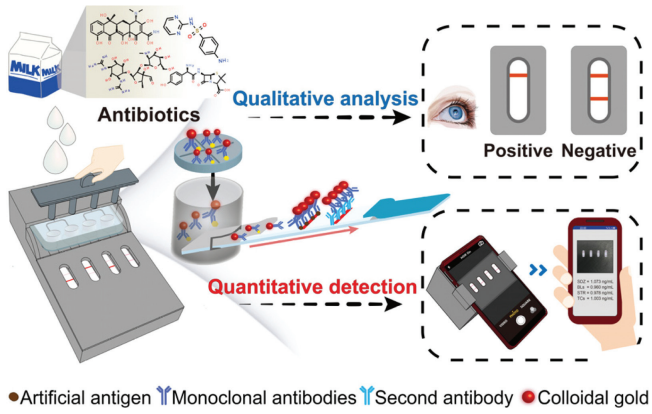

Fig. 1. Overview of the integrated microfluidic device for simultaneous detection of multiple antibiotics in milk.

In this work, we developed an integrated microfluidic device for the simultaneous detection of multiple antibiotic residues in milk using rapid qualitative and quantitative analysis (Fig. 1). Additionally, we selected four antibiotics, namely, sulfadiazine (SDZ) from sulfonamides (SAs), ampicillin (AMP) from β-lactams (BLs), streptomycin (STR), and tetracycline (TC).

The microfluidic device was created using 3D printing combined with polydimethylsiloxane (PDMS) cross-shaped slits and immunochromatographic strips to develop an immunoassay device. The device includes a customized instrument, an integrated microfluidic chip, test strips, and an image acquisition device, allowing for multiple results from a single injection (Fig. 1). Four freeze-dried colloidal gold-labeled monoclonal antibodies (CG-mAbs) were stored in the reaction wells of the microfluidic chip, each of which was used for the detection of one antibiotic. Based on the principle of indirect immune competition, the milk samples were first mixed with four CG-mAbs. If no residual antibiotics were present in the milk sample, the CG-mAbs would combine with the artificial antigens on each T-line to form red bands. Conversely, the CG-mAbs would first bond with the antibiotics in the sample. Thereafter, the free CG-mAbs would bind to the artificial antigens, and the color intensity of the T-lines would relatively weaken until the color disappeared completely. The detection device was inserted into the image acquisition device (Fig. S1 in Supporting information) after the detection, and a mobile phone application was used for image acquisition and quantitative analysis (Fig. S2 in Supporting information).

The integrated microfluidic system has four microchannels (for conveying the liquid) and four reaction wells, which can be inserted into the detection device (Fig. 2A). Cruciform slits were cut with a scalpel at the corresponding positions at the bottom of each reaction chamber. The cross-shaped structure is a valve that can be controlled by an external force (Fig. 2B). Owing to the elasticity of the silicone rubber of PDMS, the incisions created by cutting do not cause solution leakage without an external force [27]. When an external force is applied to the structure in the vertical direction, the silicone rubber is punctured, and the solution flows downward (Figs. 2B and C). An external force is applied through four small rods and simultaneously acts on the four cruciform valves. The head of this small rod is thin; the remaining rod is not a smooth cylinder and has four mutually perpendicular edges, which can open the gap of the chip valve with sufficient space for the liquid to flow (Fig. 2D). The sample is injected into the chip and pumped into the reaction chamber simultaneously through a microchannel with four equal divisions. Notably, the sample volume flowing into the four reaction wells is the same (200 μL) throughout.

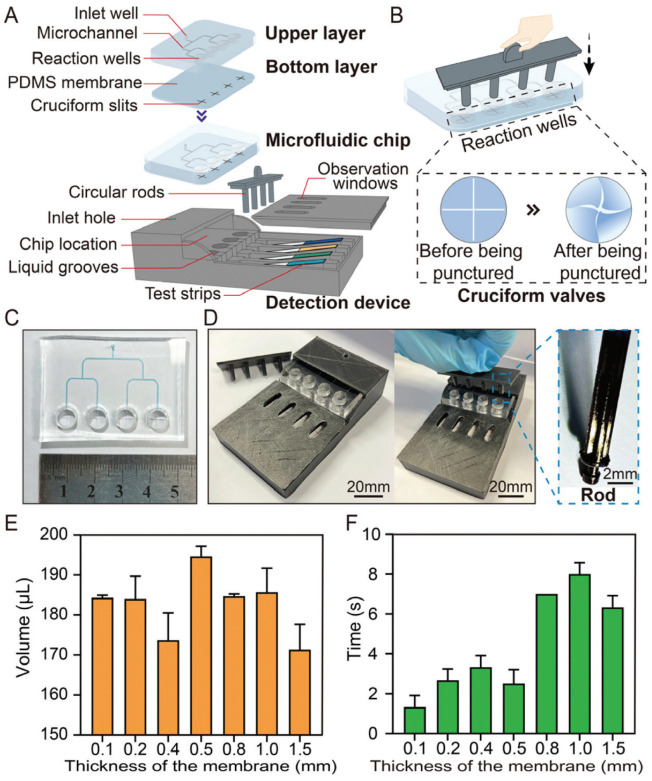

Fig. 2. Microfluidic chip and detection device. (A) Composition of the microfluidic chip and device. (B) Cruciform valve and its state before and after it was punctured. (C) Photo of the microfluidic chip. (D) Photos of the detection device and details of the circular rod. (E) Relationship between the thickness of the PDMS membrane and the volume of the solution flowing down ($n = 3$). (F) Relationship between the thickness of the PDMS membrane and flowing time ($n = 3$).

We first verified that the adsorption between the PDMS and protein would not affect the binding of antigens and antibodies and confirmed that it was feasible to use PDMS as a detection carrier (Fig. S3 in Supporting information). Next, the assay device, including the thickness of the PDMS membrane, reaction time, and inclination of test strips, were optimized.

The thickness of the PDMS membrane is important for the performance of the cruciform valves because it has a significant impact on the deformation and recovery of the PDMS membrane. To optimize the membrane thickness, PDMS membranes of different thicknesses (0.1, 0.2, 0.4, 0.5, 0.8, 1.0, and 1.5 mm) were selected. Thereafter, 200 μL of the solution was added to each chamber. After 5 min, the bottom valves were punctured vertically downward with small rods, and the volume of the solution flowing down and the time taken for the liquid to flow down were recorded. As shown in Figs. 2E and F, when the thickness is 0.1–0.5 mm, the upper solution can flow to the lower layer in a shorter time (1–3 s). PDMS membranes with a thickness of less than 0.2 mm usually cannot withstand the solution for more than 5 min; therefore, a thickness of 0.5 mm was chosen as the optimal thickness of the membrane.

To obtain the optimal reaction time, standard solutions (1.0 ng/mL) of each antibiotic were incubated with their CG-mAbs for 3, 5, 7, 10, and 15 min, and the chromatography durations were set to 3, 5, 7, 10, and 15 min, respectively. A comparison of the results showed that prolonged incubation and chromatography time (7–15 min) resulted in significantly lower detection concentrations and accurate concentrations; the longer the duration, the lower the concentrations (Figs. 3A–D). This phenomenon is due to the non-specific binding of antigens and antibodies, leading to false-negative results. However, owing to the different affinities of anti-

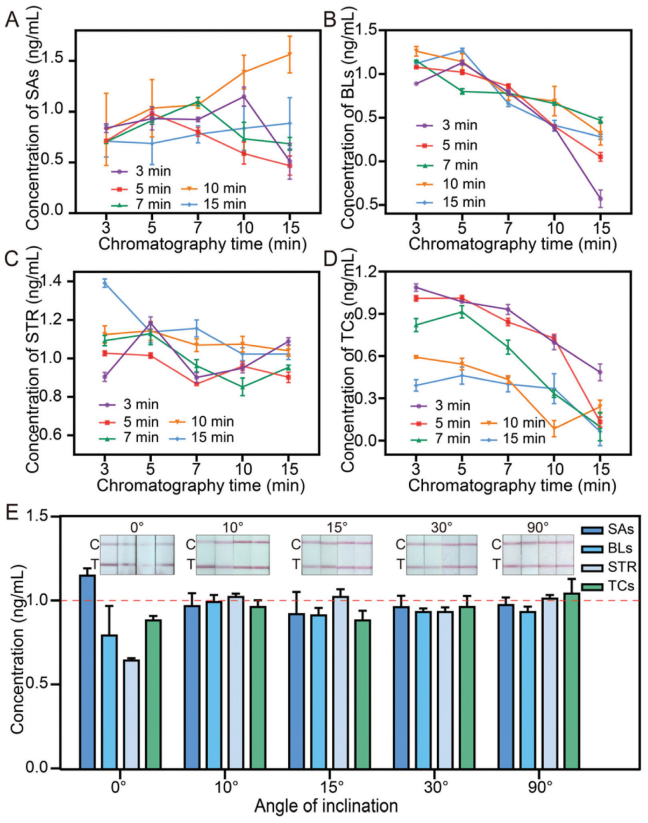

Fig. 3. Detection time and angle of inclination optimization. Relationship between the detection effect and incubation and chromatography time (SAs (A), BLs (B), STR (C), and TCs (D)). The purple, red, green, orange and blue dots represent incubation times of 3, 5, 7, 10, and 15 min, respectively. (E) Optimization of the angle of inclination of test strips. The red dotted line indicates the concentration of antibiotics of 1.0 ng/mL.

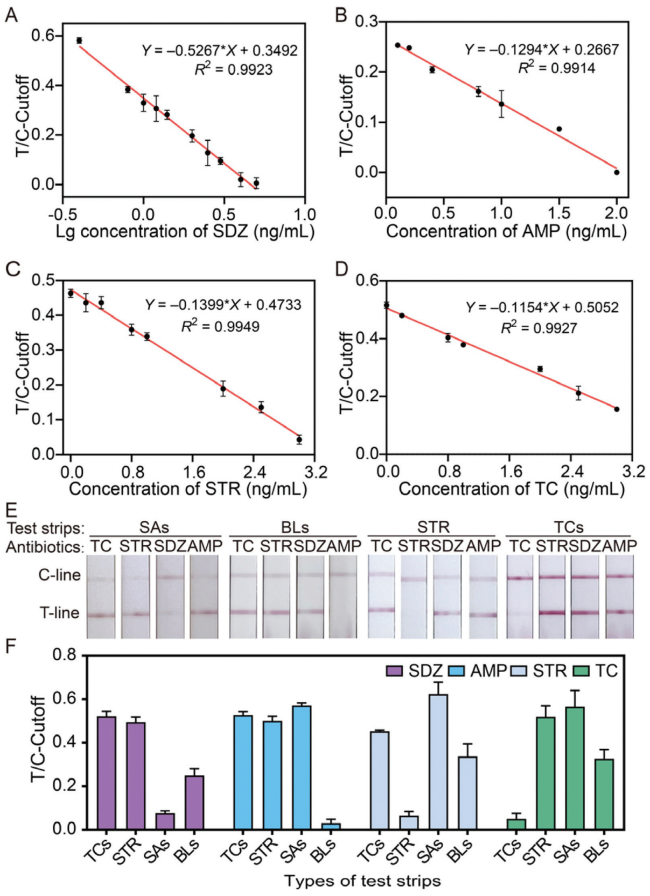

Fig. 4. Standard curves and specificity. Antibiotic detection standard curves of SAs (A), AMP (B), STR (C), and TCs (D). (E) Photos of the results of the specificity of the detection device. (F) Column chart of the results of the specificity.

gens and antibodies, when the incubation time was 3 min, the detection accuracy of the different antibiotics was different. When the incubation and chromatography times were both 5 min, the detection results were stable at 1 ng/mL; thus, for both incubation and chromatography times, 5 min was selected as the optimal time for the detection reaction.

To verify the influence of the inclination angle of the test strips, inclinations of 0°, 10°, 15°, 30°, and 90° were selected to detect the four antibiotics (1.0 ng/mL). When the test strip was inserted horizontally (0°), the solution was easily immersed in the front end of the nitrocellulose (NC) membrane, thereby affecting the binding of CG-mAbs to the artificial antigens and impacting the chromatography effect. In comparison, an inclination of 10°−90° ensured a stable detection effect (Fig. 3E). Therefore, the minimum inclination angle (10°) was chosen as the final choice given the miniaturization of the device.

The performance of the detection device was tested using a standard solution of four antibiotics (SDZ, AMP, STR, and TC). With an increase in the antibiotic concentration, the signal intensity of the T-line gradually decreased and disappeared completely. Naked-eye observations when the T-lines disappeared completely showed that the SDZ, STR, and TC concentrations were all 6.0 ng/mL, and the AMP concentration was 2.0 ng/mL. For the quantitative analysis, the T and C lines were photographed using an image acquisition platform and the change in color intensity was analyzed. To establish a standard curve for each antibiotic, the T/C-cutoff was used as the *y*-axis, the logarithmic concentration of the antibiotic as the *x*-axis for sulfadiazine (SDZ), and the antibiotic concentration as the *x*-axis for the other three antibiotics (AMP, STR, and TC) (Figs. 4A–D and Fig. S4 in Supporting information). The cutoff value was defined as the ratio of the signal intensity of the T-line to the C-line (T/C), corresponding to the minimum concentration of antibiotics causing the T-line to disappear. All four antibiotics displayed excellent linear relationships, with linear correlation coefficients (R^2) above 0.99. The linear ranges of each antibiotic were 0.4–5.0 ng/mL for SDZ, 0.1–2.0 ng/mL for AMP, and 0–3.0 ng/mL for STR and TC. The limits of detection (LODs) of each antibiotic were calculated as $LOD = 3\sigma/k$, where σ is the standard deviation of the signal value of the negative sample taken six times, and k represents the slope of the standard curve. The LOD values were 0.15, 0.12, 0.25, and 0.29 ng/mL for SDZ, AMP, STR and TC, respectively, and were lower than the MRLs specified by WHO.

To evaluate the specificity of the assay, the standard solutions of the four antibiotics were added to the negative milk samples, incubated with CG-mAbs, and detected with the corresponding test strips. The concentrations of the four representative antibiotics (SDZ, AMP, STR, and TC) corresponded to the cutoff values. When SDZ is detected, the signal value is the lowest, the T-line disappears and is positive, and the signal values of AMP, STR, and TC are high and negative, indicating that there is good specificity for SDZ in one of the channels (Figs. 4E and F). Similarly, when AMP is detected, the signal value is the lowest, the T-line disappears and is positive, and the signal values of SDZ, STR, and TC are higher and negative, indicating that the other channel of the four channels is specific for AMP. STR and TC were detected under the same conditions. When the corresponding antibiotic was detected, the signal value was the lowest (positive, T-line disappeared). By contrast, the signal value for other antibiotics was higher (negative), indicating that the device had excellent specificity.

To determine the feasibility, portability, on-site detection capability, and remote data processing capability of our detection system, multiple antibiotic tests were performed on milk from three dairy industries in China (Yili skim milk, Mengniu fresh milk, and Bright Dairy fresh milk). These samples were also verified to be negative using ELISA (Table S1 in Supporting information). Antibiotic solutions containing SDZ (1, 2, 2.5 ng/mL), AMP (1, 1.5, 2.5 ng/mL), STR (1, 2, 2.5 ng/mL), and TC (1, 2, 2.5 ng/mL) were added to each sample. The spiked samples were then injected into the microfluidic chip from the inlet well, and the sample solutions flowed into the reaction wells through the microchannel to react with CG-mAbs. The samples were detected using lateral flow immunoassay strips. Each sample was tested in triplicate, and the results are summarized in Table S2 (Supporting information). The average recoveries of the four antibiotics in all the samples ranged from 91.92% to 108.29%, and the coefficient of variation was less than 10% ($n = 3$), indicating that the detection device has good reproducibility and accuracy and can be used for the quantitative analysis of antibiotic residues. Thus, it is suitable for on-site detection, and the detection results can be shared in time, which is conducive for rapid and efficient responses by regulatory authorities and users.

In conclusion, an integrated immunochromatographic microfluidic device was developed in this work. The microfluidic chip contained cruciform valves, which controlled the flow of liquids. This device was used to simultaneously detect four types of antibiotics (SAs, BLs, STR, and TCs) in milk. The LODs for SDZ, AMP, STR, and TC were 0.15, 0.12, 0.25, and 0.29 ng/mL, respectively, which are much lower than the MRLs stipulated by the European Union and WHO (0–5, 0.1–2, 0–3, and 0–3 ng/mL, respectively). The average recovery rates of the antibiotics in milk were between 91.92% and 108.29%, and the detection time was maintained within 10 min. This indirect immunoassay method has the advantages of low cost, fast detection, and portability and can be used for detecting antibiotics in the field of food safety. Furthermore, by designing microfluidic chips with more channels, this detection platform could potentially detect a more extensive range of target compounds.

Declaration of competing interest

The authors declare no conflict of interest.

Acknowledgments

This work was supported financially by the National Natural Science Foundation of China (Nos. 82073816 and 21727814), and Advanced Talents of Beijing Technology and Business University (No. 19008021179).

Supplementary materials

Supplementary material associated with this article can be found, in the online version, at doi:10.1016/j.cclet.2022.108110.

References

[1] D. Bitas, A. Kabir, M. Locatelli, V. Samanidou, Separations 5 (2018) 31.
[2] A. Boobis, C. Cerniglia, A. Chicoine, V. Samanidou, Crit. Rev. Toxicol. 47 (2017) 889–903.
[3] Q. Wang, Q. Xue, T. Chen, et al., Chin. Chem. Lett. 32 (2021) 609–619.
[4] L. Maier, C.V. Goemans, J. Wirbel, et al., Nature 599 (2021) 120–124.
[5] T. Ramatla, L. Ngoma, M. Adetunji, M. Mwanza, Antibiotics 6 (2017) 34.
[6] Z. Aversa, E.J. Atkinson, M.J. Schafer, et al., Mayo Clin. Proc. 96 (2021) 66–77.
[7] A. Aidara-Kane, F.J. Angulo, J.M. Conly, et al., Antimicrob. Resist. Infect. Cont. 7 (2018) 7.
[8] M. Chen, R. Luo, S. Li, et al., Anal. Chem. 92 (2020) 13336–13342.
[9] R. De O. Silva, M.G.G. De Menezes, R.C. De Castro, et al., Food Chem. 297 (2019) 124934.
[10] M. Han, L. Gong, J. Wang, et al., Sens. Actuators B: Chem. 292 (2019) 94–104.
[11] T. Li, C. Wang, Z. Xu, A. Chakraborty, Chemosphere 254 (2020) 126765.
[12] Q. Shi, J. Huang, Y. Sun, et al., Spectrochim. Acta A 197 (2018) 107–113.
[13] B. Al Mughairy, H.A.J. Al-Lawati, Trends Anal. Chem. 124 (2020) 115802.
[14] M. Pucetaite, P. Ohlsson, P. Persson, E. Hammer, Soil. Biol. Biochem. 153 (2021) 108078.
[15] Z. Wu, L. Lin, Chin. Chem. Lett. 33 (2022) 1752–1756.
[16] J.M.D. Machado, R.R.G. Soares, V. Chu, J.P. Conde, Biosens. Bioelectron. 99 (2018) 40–46.
[17] H.K. Li, H.L. Ye, X.X. Zhao, et al., Chin. Chem. Lett. 32 (2021) 2851–2855.
[18] W. Qi, L. Zheng, Y. Hou, et al., Food Chem. 381 (2022) 131801.
[19] G. Xing, W. Zhang, N. Li, et al., Chin. Chem. Lett. 33 (2022) 1743–1751.
[20] M. Zhang, J. He, Y. Chen, et al., Chin. Chem. Lett. 31 (2020) 2721–2724.
[21] Q. Zhang, S. Feng, L. Lin, S. Mao, J.M. Lin, Chem. Soc. Rev. 50 (2021) 5333–5348.
[22] W. Zhang, N. Li, L. Lin, et al., Small 16 (2020) 1903402.
[23] L. Lin, L. Yi, F. Zhao, et al., Chem. Sci. 11 (2020) 2744–2749.
[24] Y. Zheng, Z. Wu, J.M. Lin, L. Lin, Chin. Chem. Lett. 31 (2020) 451–454.
[25] Z. Su, W. Hu, L. Ye, D. Gao, J.M. Lin, Chin. Chem. Lett. 34 (2023) 107790.
[26] L. Huang, E. Su, Y. Liu, et al., Chin. Chem. Lett. 32 (2021) 1555–1558.
[27] Y. Shi, M. Hu, Y. Xing, Y. Li, Mater. Des. 185 (2020) 108219.